

# Self-Oscillatory Neck Propagation in Polymers

Sergey Bazhenov

*Institute of Synthetic Polymeric Materials, Russian Academy of Sciences, Moscow 117393, Russia*

Received 7 July 2009; accepted 27 April 2010

DOI 10.1002/app.32804

Published online 27 July 2010 in Wiley Online Library (wileyonlinelibrary.com).

**ABSTRACT:** The oscillatory neck propagation during cold drawing of PET was studied. The mechanism of self-oscillations is heat instability of neck propagation. Oscillations are observed at high velocities when the draw stress increases with an increase in cross-head speed. Neck propagation is described by three equations, which were solved numerically. The solution of these equations predicts appearance of oscillations at high elongation velocities in

agreement with experimental observations. The necessary condition of appearance of oscillations in any polymer is existence of some interval of cross-head speeds  $V$ , where the draw stress decreases with an increase in  $V$ . © 2010 Wiley Periodicals, Inc. *J Appl Polym Sci* 119: 654–661, 2011

**Key words:** mechanical properties; thermal properties; theory

## INTRODUCTION

The plastic yielding of polymers often starts from a localized formation of a neck followed by its propagation through the sample. The neck usually propagates at a constant draw stress. However, in amorphous polyethyleneterephthalate (PET) at constant cross-head speed oscillations of tensile stress were observed.<sup>1,2</sup> The stress oscillations are related with oscillations of temperature and yielding velocity in the neck.<sup>3</sup> The local temperature in a neck reaches 90–140°C. This value exceeds the glass transition temperature of PET ( $\approx 75^\circ\text{C}$ ). The growth of temperature was registered with low-molecular weight powder dusted on the surface of the sample and melted in high temperature areas.<sup>3</sup> In addition, temperature growth was registered with an infrared camera.<sup>4–6</sup>

Oscillations appear only if the length of sample exceeds some critical value.<sup>3</sup> A neck in comparatively short samples initially propagates steadily without oscillations. However, as the length of the drawn material increases, regular oscillations appear and after a time this process becomes firmly established. Oscillations in comparatively long samples appear right after initiation of the neck. The oscillatory neck propagation is rather general phenomenon observed in different linear polymers. For example, in PET, PVC, PA-6, PP, and HDPE.<sup>7</sup> However, the

critical sample length of appearance of oscillations depends on polymer.

In PET and PVC, the critical length is 5–30 mm; while for PP and HDPE, it is 0.9 and 7 m, respectively.<sup>7</sup> The critical length for PP and HDPE is so high that oscillations are observed only if a sample is tested in consequence with a spring. Spring accumulates elastic energy and models testing of long samples. Total energy stored by a sample and a spring is described by the compliance of the system. According to Kechejian, Andrianava, and Kargin, in PET oscillations appear if the compliance of the system (a sample and a spring) exceeds the critical value.<sup>3</sup> The compliance of a sample is proportional to its length (for elastic material  $D = L/E$ , where  $L$  is the length of the sample, and  $E$  is elastic modulus of the material).

On the first sight, it seems that oscillations may be observed in any polymer yielding by propagation of a localized neck if a sample is tested in consequence with a spring. However, in polycarbonate a localized neck is formed but oscillations do not appear. The reason is not clear.

Mechanism of self-oscillations is discussed. Two alternative mechanisms of self-oscillatory neck propagation are proposed. The first is heat instability related with growth of temperature in a narrow transitional region between the neck and the non-oriented polymer.<sup>3</sup> Heating is caused by mechanical work produced by testing machine and converted into heat in the narrow transitional region. An alternative mechanism of self-oscillations is crystallization of PET in neck.<sup>8,9</sup>

Barenblatt introduced a model of a transitional region between the neck and non-oriented polymer and assumed that orientation and conversion of

Correspondence to: S. Bazhenov (bazhenov\_sl@rambler.ru).

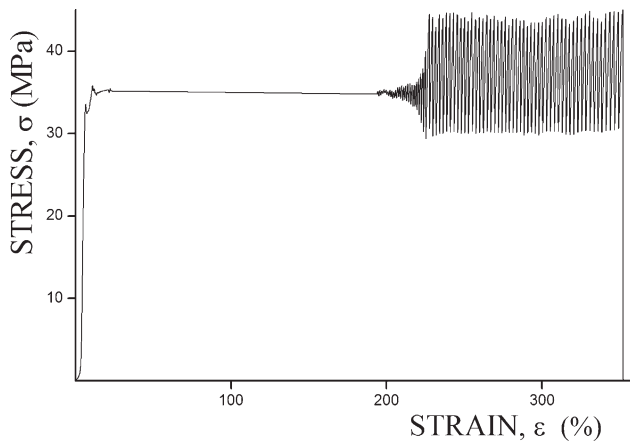


**Figure 1** Typical stress-strain curve of oscillatory neck propagation in PET.

mechanical work into heat occurs in this region.<sup>10</sup> Temperature of the transitional region and tensile stress were described by two first order differential equations, and self-oscillations were explained by instability of temperature and stress at neck propagation.<sup>10</sup> Barenblatt's theory was developed further and an analytical criterion of appearance of oscillations was derived.<sup>11</sup> The comparison of the theory and experiment revealed their dramatic disagreement.<sup>12</sup>

The period of oscillations in PET at the later stage of drawing usually becomes doubled.<sup>3</sup> To explain the period doubling, Toda described temperature of a polymer with the modified heat diffusion equation.<sup>13</sup> The goal of this article is modification of Toda's equations and quantitative comparison of the theory with experimental data to prove thermal mechanism of self-oscillations in PET.

## EXPERIMENTAL

Commercial films of amorphous non-oriented PET were tested in tension. The thickness of the film was 170  $\mu\text{m}$ . Samples were straight strips cut from the film. The width of samples was 5 mm, and their gage length was varied from 5 to 100 mm. To initiate necking, samples before testing were plastically bent in their center. Oscillations appeared during propagation of the neck. Samples were tested at room temperature with a cross-head speed of 0.01–1000 mm/min with a Shimadzu Autograph AGS-H universal testing machine.

To measure the critical compliance  $D_c$ , sample was drawn until the appearance of regular oscillations. After that it was unloaded and loaded again to determine the slope of the initial linear part of the stress-elongation curve. The critical compliance  $D_c$  was calculated from the slope as  $D_c = \Delta L / \Delta\sigma$ ; where  $\Delta L$  is the increment of the sample length, and

$\Delta\sigma$  is the increment of the engineering stress. The critical length of unnecked samples was calculated with the equation  $L_c = D_c E$ , where  $D_c$  is the determined critical compliance of samples and  $E = 4$  GPa is the Young's modulus of PET. Results of testing of 4 samples were averaged.

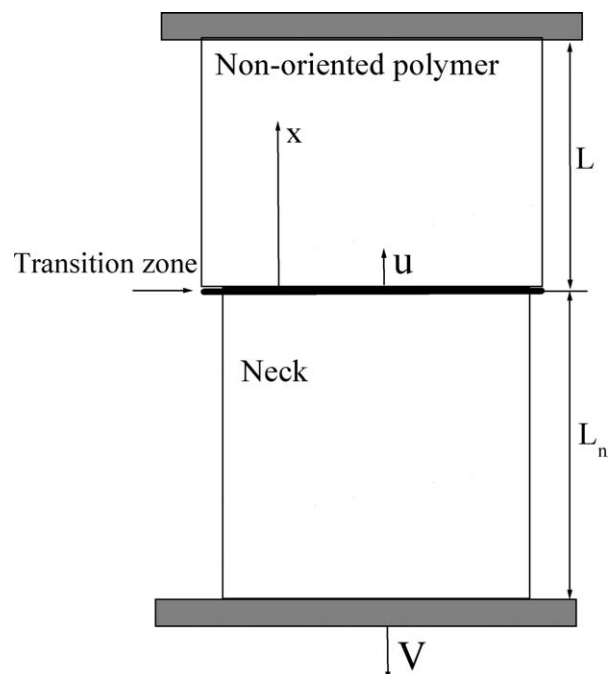
The draw stress was measured by tensile testing of short samples when neck propagation was stable. To measure the draw ratio of PET in a neck, several points were painted with a marker at a distance of 3 mm along the work part of samples. The test machine was stopped when the neck passed these points. The draw ratio was measured as  $\lambda = L_1 / L_0$ , where  $L_0$  and  $L_1$  are the initial and the final distance between the points.

Samples were photographed with a Canon EOS 20D camera. In addition, samples were fractured along the neck propagation direction in liquid nitrogen, and the fracture surface was examined with a Hitachi S-520 scanning electron microscope (SEM).

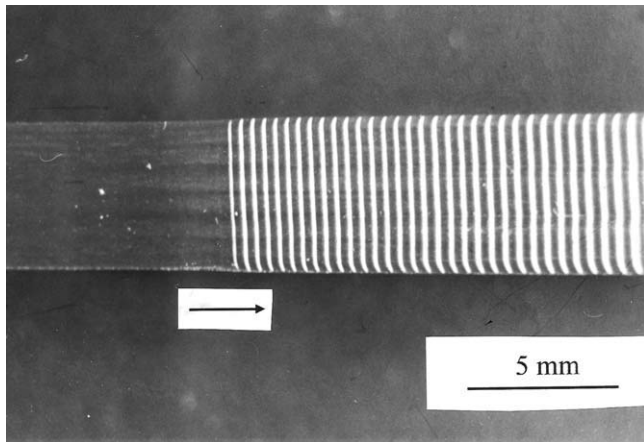
## RESULTS

Figure 1 shows a typical PET tensile stress  $\sigma$  – strain  $\varepsilon$  curve. The neck initially propagated steadily without oscillations. However, at strain  $\varepsilon \approx 220\%$  regular oscillations in stress appeared.

Figure 2 shows schematic drawing of a neck propagating along a sample in the coordinate system related with the upper grip of the testing machine. On the Figure, the upper grip and non-oriented part of the sample do not move, and the speed of the



**Figure 2** The model of a necked sample.  $V$  and  $u$  are the cross-head speed and the neck propagation velocity.

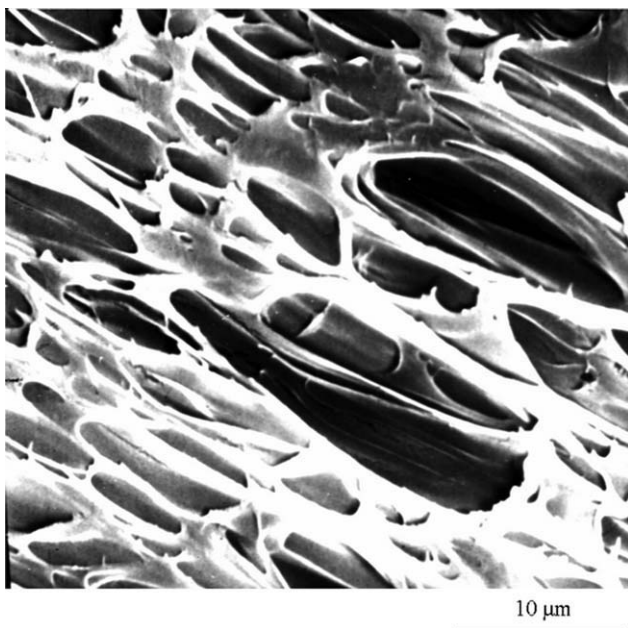


**Figure 3** The photograph of a neck in PET drawn at cross-head speed 50 mm/min. The arrow shows the direction of the neck propagation.

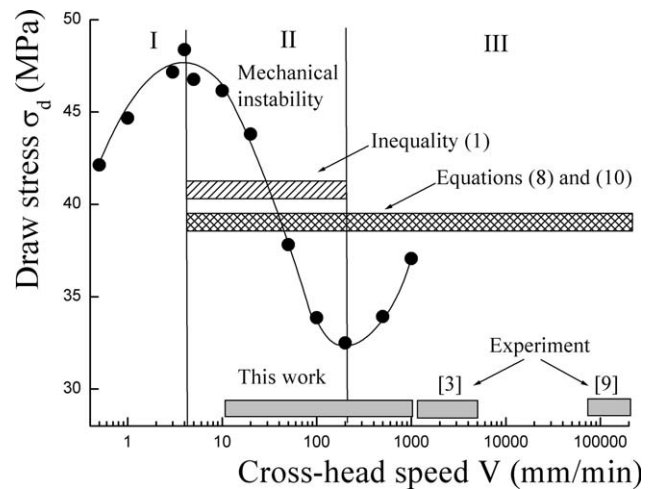
lower grip and the neck is  $V$ . The neck propagation velocity  $u$  is the velocity of the boundary between the neck and non-oriented parts of the sample.

Figure 3 shows photograph of the neck in PET film. The arrow shows the direction of the neck propagation. Initiation of oscillations leads to appearance of alternating white and dark bands in the neck. White bands correspond to fast neck propagation when the temperature of the transitional zone is high. Figure 4 shows the structure of white bands in a scanning electron microscope. In the white band a number of voids are observed. The voids scatter light and are white on the Figure 3.

Figure 5 shows the draw stress  $\sigma_d$  of PET plotted against the cross-head speed  $V$ . The plot of the draw



**Figure 4** The SEM micrograph of pores in PET white bands.



**Figure 5** The draw stress  $\sigma_d$  plotted against the cross-head speed  $V$ . Rectangles show the intervals of oscillatory neck propagation observed in experiments and predicted by Inequality (1) and eqs. (8), (10), and (11).

stress is described by an N-shape curve. At low  $V$  (in the region I)  $\sigma_d$  increases with an increase in  $V$ . In contrast, at medium cross-head speeds (in the region II)  $\sigma_d$  decreases with  $V$ , and at high  $V$  (in the region III) it increases again. The decrease of  $\sigma_d$  in the region II is caused by the growth of temperature with an increase in  $V$ . The classical criterion of mechanical instability in this region of cross-head speeds is fulfilled<sup>14</sup>:

$$\frac{d\sigma}{dV} < 0 \quad (1)$$

Oscillations are expected in the region II in Figure 5. However, oscillatory neck propagation in PET is observed both in the regions II and III. Figure 5 shows the cross-head speed region where the neck propagation is oscillatory. In this work, oscillations were observed at speeds from 10 to 1000 mm/min, the highest cross-head speed of the Shimadzu testing machine. At  $V < 120$  mm/min stress oscillations are registered with the testing machines. However, at higher cross-head speeds oscillations appear but the test machine does not register them due to insufficient time resolution. Occasionally, the minimum of the draw stress in Figure 5 is observed at speeds close to  $V \approx 120$  mm/min. On this reason, the author earlier erroneously concluded that Inequality (1) determines the speed interval where oscillations may appear.<sup>11</sup> However, in PET oscillations exist at higher  $V$ , in the region III in Figure 5.

There are two ways to register oscillations at high cross-head speeds. The first is to record stress oscillations with an oscilloscope<sup>3</sup> or an impact test equipment.<sup>9</sup> The second method is visual checking if alternating white and dark bands are observed in the neck. Figure 6 shows the photograph of the PET

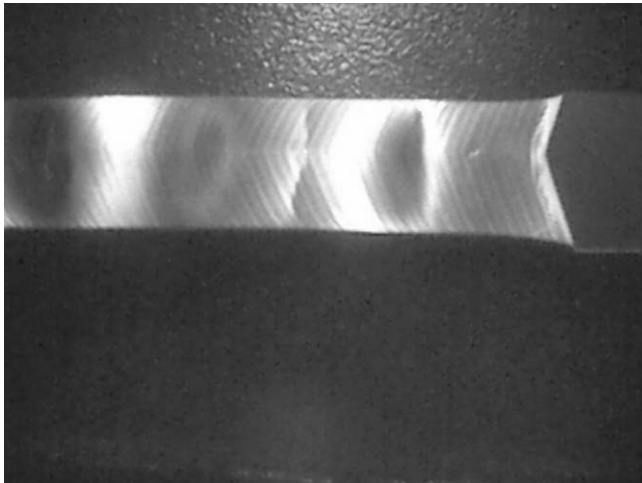


**Figure 6** The photograph of the PET film drawn at 1000 mm/min cross-head speed. The neck propagated from left to right. The neck front is not straight and the neck is buckled due to heating.

film drawn at cross-head speed of 1000 mm/min. Alternating dark and light bands reveal existence of oscillations. It is worth mentioning that at this velocity the neck front was angle-shaped. Stress oscillations in PET were registered with an oscilloscope at the cross-head speed of  $V = 5000$  mm/min,<sup>3</sup> and with an impact equipment at  $V = 72$  and 220 m/min.<sup>9</sup>

The mechanism of oscillations in PET is different from simple mechanical instability, the criterion of which is described by Inequality (1). To explain appearance of oscillations in the region III in Figure 5, below equations describing self-oscillatory neck propagation are derived. These equations are similar to the Barenblatt-Toda's equations modified to consider the effect of the draw ratio  $\lambda$  on the heating of a polymer.

Figure 7 shows the draw ratio  $\lambda$  in neck plotted against the cross-head speed  $V$ . The draw ratio is equal to 4 if  $V < 70$  mm/min, and increases at higher  $V$ . Below an increase in  $\lambda$  was neglected.

**Basic equations**

**Stress**

Assuming that polymer behavior is linear elastic everywhere but for the negligibly thin transitional region between the neck and the non-oriented part of the sample (Fig. 2), elastic elongation is given by:

$$\Delta L_e = \frac{L\sigma}{E} + \frac{L_n\sigma_n}{E_n} = D\sigma, \tag{2}$$

where subscript n corresponds to the neck,  $L$  and  $L_n$  represent the lengths of the non-oriented and necked parts of the sample,  $E$  elastic modulus and  $\sigma$  stress,

$D$  compliance of the sample. Stress in neck  $\sigma_n$  is given by:

$$\sigma_n = \frac{S}{S_n}\sigma = \lambda\sigma, \tag{3}$$

where  $\lambda = S/S_n = L_n/L_0$  is the draw ratio of the polymer in neck, and  $L_0$  is its initial length. Hence, compliance is determined by Equation:

$$D = \frac{L}{E} + \frac{\lambda L_n}{E_n} \tag{4}$$

Total elongation of a sample is equal to the sum of elastic and plastic components:

$$\Delta L = \Delta L_e + \Delta L_p \tag{5}$$

Derivative of this equation is:

$$V = \dot{\epsilon}_e + \dot{\epsilon}_p \tag{6}$$

where  $V = \frac{d\Delta L}{dt}$  is the cross head speed (Fig. 2),  $\dot{\epsilon}_e = \frac{d\Delta L_e}{dt}$  and  $\dot{\epsilon}_p = \frac{d\Delta L_p}{dt}$  - velocities of elastic and plastic deformations.

If the transitional region velocity is  $u$ , the decrease of the length of non-oriented part of sample for time  $dt$  is  $u dt$  and the increment of the neck length is  $u\lambda dt$ . Hence the increment of the plastic elongation  $dL_p$  is:

$$dL_p = (\lambda - 1) u dt \tag{7}$$

Combination of eqs. (2), (6), and (7) gives:

$$\frac{d\sigma}{dt} = \frac{V - (\lambda - 1)u}{D} \tag{8}$$

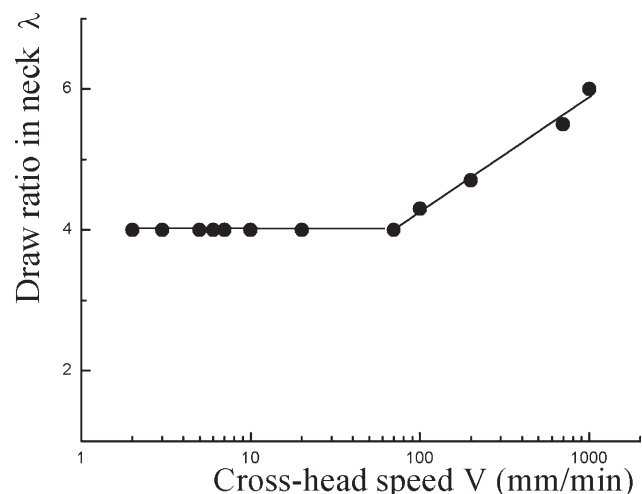


**Figure 7** The PET draw ratio in neck  $\lambda$  plotted against the cross-head speed  $V$ .

If the neck does not move,  $u = 0$  and eq. (8) corresponds to the Hooke's law at constant cross-head speed  $V$ . If  $u \neq 0$ , plastic strain  $\varepsilon_p$  replaces elastic strain  $\varepsilon_e$  and the stress-strain curve deviates from linear.

At  $\lambda = 2$  eq. (8) coincides with that used by Barenblatt<sup>10</sup> and Toda.<sup>13</sup> However, typical value of  $\lambda$  for PET is from 4 to 6 (Fig. 7).

### Temperature

Putting the origin of the coordinate system in the moving transitional region as shown in Figure 2, Toda described temperature of polymer by equation<sup>13</sup>:

$$\rho c \frac{\partial T}{\partial t} = k \frac{\partial^2 T}{\partial x^2} - \rho c u \frac{\partial T}{\partial x^2} - \beta \left( \frac{1}{w} + \frac{1}{h} \right) (T - T_0), \quad (9)$$

$$+ \frac{S}{\omega} \sigma u \quad \text{for } 0 \leq x \leq \Delta x.$$

where  $T(x, t)$  and  $T_0$  represent temperatures of a polymer and a surrounding air respectively,  $\rho$  density,  $c$  heat capacity,  $k$  and  $\beta$  the thermal conductivity of the polymer and the heat transfer coefficient to the surrounding air ( $Q = \beta S_1 (T - T_0)$ ),  $w$  and  $h$  the width and the thickness of the sample,  $x$  the direction of neck propagation,  $S$  the original cross-sectional area,  $Q$  the heat transferred to the surroundings,  $\omega$  and  $S_1$  the volume and surface area of the transitional region.

The first and the second terms on the right-hand side of eq. (9) are heat conductivity equation in moving coordinate system, the third term describes the heat transfer from the polymer to the surrounding air, and the last term describes the heat produced in the transitional zone per unit time. Below the last term describing heat produced in the transition region is corrected.

If the neck propagates steadily with a constant velocity  $u$ , the produced mechanical work is equal to a product of the applied force and the increment in plastic elongation  $dA = F dL_p$ . Taking into account eq. (7),  $dA = F (\lambda - 1) u dt$  and the produced mechanical work is  $\sigma w h (\lambda - 1) u$ . If the fraction of mechanical work converted into heat is  $\alpha$ , and the thickness of sample  $h$  is negligible in comparison with its width  $w$ , and polymer temperature is described by Equation:

$$\frac{\partial}{\partial t} = a^2 \frac{\partial^2 T}{\partial x^2} + u \frac{\partial T}{\partial x} - \frac{2\beta(T - T_0)}{\rho c h} + \delta(x) \frac{\alpha(\lambda - 1)\sigma u}{\rho c} \quad (10)$$

where  $a = \sqrt{\frac{k}{\rho c}}$ ,  $\delta(x)$  the Dirac's  $\delta$ -function and coefficient 2 in the third term on the right-hand side of eq. (3) accounts for two surfaces of a film.

According to Ref. 15 for PET  $\alpha$  is close to 1 and almost all produced mechanical work is converted into heat. Coefficient  $\alpha$  depends on polymer and cross-head speed, varying from 0.6 to 1.12. The typical  $\alpha$  value for different polymers is  $\approx 0.8$ . The heat may exceed produced mechanical work due to latent crystallization heat. For PET  $\alpha$  varies from 0.86 to 1.12, and calculations were performed for  $\alpha = 1$ .

Following<sup>11,13</sup>, the rate of plastic deformation in the transitional zone is described by the Eyring equation:

$$u(t) = \dot{\varepsilon}_0 h \exp\left(\frac{a\sigma - U}{RT}\right), \quad (11)$$

where  $\dot{\varepsilon}_0 \approx 10^{13}$ ;  $U$  is the activation energy;  $a$  is the activation volume of the drawing process;  $R = 8.31$  J/(K mol) is the gas constant;  $T$  is the temperature of the transitional region where the polymer is yielding.

### Method of calculation

Tensile drawing of a PET sample with constant cross-head speed was modeled by numerical solution of eqs. (8), (10), and (11) at  $V = \text{Const}$ ,  $\alpha = 1$  and different draw ratios  $\lambda$ . The surrounding air temperature  $T_0$  was 20°C, the cross-head speed  $V$  was changed from 0.01 to 1000 mm/min. The boundary conditions were  $T|_{x \rightarrow \infty} = 0$  and  $T|_{x \rightarrow -\infty} = 0$ . The compliance of samples and draw ratio  $\lambda$  at calculations were constants.

The following values of the PET properties<sup>11</sup> were used:  $\rho = 1332$  kg m<sup>-3</sup>;  $k = 0.14$  Wt m<sup>-1</sup>K<sup>-1</sup>;  $c = 1300$  J kg<sup>-1</sup>K<sup>-1</sup>;  $E = 4$  GPa;  $\beta = 50$  Wt m<sup>-2</sup> K<sup>-1</sup>. Parameters of the Eyring equation are:  $U = 122$  kJ/mol;  $a = 8.412 \times 10^{-4}$  m<sup>3</sup> mol<sup>-1</sup>. The thickness of samples  $h = 0.17$  mm.

Equations (8), (10), and (11) were solved by the method of finite differences. Calculation procedure was the implicit four-point scheme, which is stable at all time and coordinate increments  $\Delta t$  and  $\Delta x$ . The increment of time  $\Delta t$  was varied during calculations. If the yield velocity for the time  $\Delta t$  increased by more than 2%,  $\Delta t$  was divided by 2 and data were recalculated. If the change in yield velocity for  $\Delta t$  was less than  $10^{-15}$ ,  $\Delta t$  was doubled.

For steady neck propagation  $\frac{\partial T}{\partial t} = 0$ , and the solution of eq. (10) is  $T(x) = C e^{-x/\delta}$ . The numerical solution of eq. (10) for oscillatory neck propagation was determined in 1997 points  $x_i$  for intervals  $-7\delta \leq x_i \leq 0$  and  $0 \leq x_i \leq 7\delta_1$ , where  $x_i = -7\delta + i \Delta x$ ,  $\Delta x = 7\delta/1000$  or  $\Delta x = 7\delta_1/1000$  ( $\delta$  and  $\delta_1$  correspond to non-oriented region and the neck, respectively). The temperature in the points  $x = 7\delta$  and  $x = -7\delta_1$  was put  $T = T_0$ . The accuracy of the calculation method was checked by the comparison of the temperature

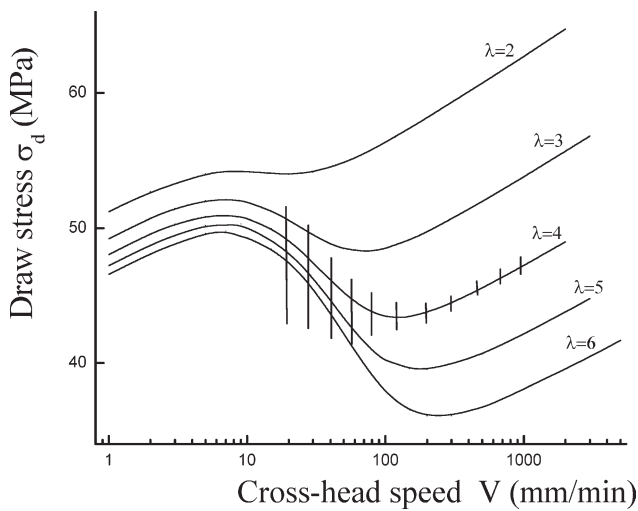


**Figure 8** The theoretical draw stress  $\sigma_d$  plotted against the cross-head speed  $V$  for  $\lambda = 2, 3, 4, 5,$  and  $6$ . The bars represent the amplitude of stress oscillations for  $\lambda = 4$ .

distribution for steady neck propagation with an analytical solution of eq. (10), and the difference was less than 0.01%.

**Numerical results**

Figure 8 shows the calculated drawing stress  $\sigma_d$  plotted against the cross-head speed  $V$  at different draw ratios  $\lambda$ . Calculations of  $\sigma_d$  were performed at low elastic compliance  $D$  when neck propagation is steady. The drawing stress for  $\lambda \leq 2$  increases monotonously with an increase in  $V$ . The shape of curves at  $\lambda > 2.1$  changes and becomes N-shaped. The draw stress  $\sigma_d$  at medium cross-head speeds decreases with  $V$ .

The drawing stress in Figure 8 decreases with an increase in the draw ratio  $\lambda$ . This is explained by more significant increase of temperature at higher draw ratios. The temperature growth at  $\lambda \leq 2$  is not significant and the draw stress monotonously increases with an increase in  $V$ . At higher  $\lambda$  lower amount of "cold" polymer comes into the transitional zone while the produced mechanical work remains the same. As a result, temperature is higher.

Figure 8 shows also the calculated amplitudes of stress oscillations for  $\lambda = 4$ . The amplitude of oscillations decreases with an increase in the cross-head speed  $V$ . Thus, theory predicts existence of oscillations both at intermediate cross-head speeds (in the region II in Fig. 5) and at high speeds (in the region III). For  $\lambda \leq 2$   $d\sigma_d/dV > 0$  at any  $V$ , and  $T, u$  and  $\sigma_d$  were steady even at very high  $D$ . Hence, oscillations appear if in some interval of cross-head speeds  $V$  stress  $\sigma_d$  decreases with an increase in  $V$  and the Inequality (1) is fulfilled. Inequality (1) is the necessary

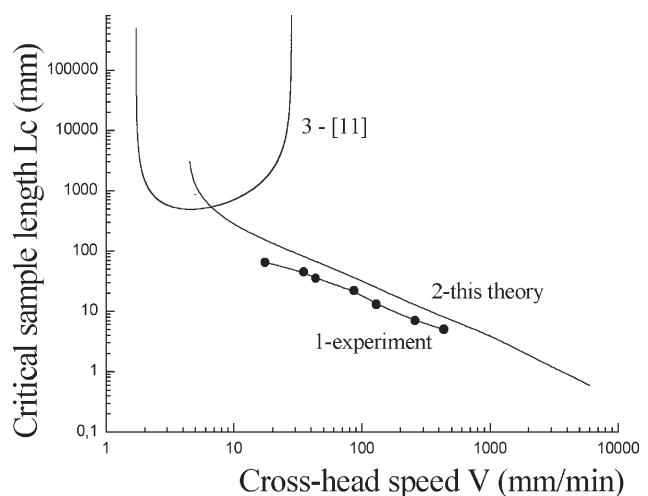
condition of oscillations appearance. However, the cross-head speed interval of oscillation is not described by Inequality (1). Oscillations are observed both at intermediate and high cross-head speeds (in the regions II and III in Fig. 5). Thus, the Inequality (1) is not the criterion of oscillations appearance; it is the necessary condition of oscillations.

Figure 9 shows the critical sample length  $L_c$  (at which the oscillations appear) plotted against the cross-head speed  $V$ . The critical length  $L_c$  decreases with an increase in  $V$ . The theoretical values of  $L_c$  for  $\lambda = 4$  (the curve 2) are approximately twice higher than the experimental ones (the curve 1). Thus, the experimental and the theoretical values of  $L_c$  are in decent agreement. Hence, eqs. (8), (10), and (11) describe the oscillatory neck propagation in PET and the mechanism of oscillations is thermal instability of neck propagation. For comparison, the curve 3 shows  $L_c$  values calculated by Bazhenov and Keckekian according to modified Barenblatt theory.<sup>11</sup> The curve 3 does not describe the experimental data.

**DISCUSSION**

The present article represents the third subsequent step in development of the theory of oscillatory neck propagation in polymers. The first step was done by Barenblatt<sup>10</sup> and the second by Toda.<sup>13</sup> To clarify the difference with these works, below Barenblatt and Toda's equations are considered. Barenblatt showed the direction of the theory development. His goal was explanation of the effect of self-oscillations and this problem was solved.

The neck propagation in polymers is similar to propagation of a flame wave. The theory of flame



**Figure 9** The critical length  $L_c$  of samples plotted against the cross-head speed  $V$ . Curve 1: experimental data; curve 2: the present theory; curve 3: modified Barenblatt theory.<sup>11</sup>

wave propagation is based on two equations: the heat diffusion equation and the diffusion equation. This theory was found in the end of XIX century by Mikhelson<sup>16</sup> and developed further by several researchers. The main results are described in the book "Mathematical theory of combustion and explosion," and Barenblatt is its co-author.<sup>18</sup> However, Barenblatt did not apply the classical flame propagation theory to the neck propagation and developed a model simplifying the heat diffusion equation.<sup>10</sup> As a result, neck propagation was described by two differential equations:

$$\frac{d\sigma}{dt} = \frac{V - u}{D}, \quad (12a)$$

$$\frac{dT}{dt} = q - \xi(T - T_0), \quad (12b)$$

where  $q = \frac{Q}{c} - \frac{1}{\gamma d}u(T - T_0)$ ;  $d$  is the thickness of the transitional zone;  $\xi = \frac{\beta S}{\rho c}$ ;  $\gamma$  is the coefficient, corresponding to the shape of the transitional zone (its value is close to unity).

Analysis of stability of eqs. (12a) and (12b) is simple. This was done in<sup>11</sup> and the results of calculation of the critical sample length  $L_c$  for PET are shown by the curve 3 in Figure 9. The theoretical and experimental values of  $L_c$  disagree, and the author erroneously concluded that the nature of phenomenon is not clear.<sup>12</sup>

The present work shows that the disagreement is caused by the inaccuracy of eq. (12b). Usually mathematically incorrect methods give quite close approximate solution of a problem. However, this case is the exclusion and eq. (12b) can not be used for analysis of neck propagation stability.

Equation (8) corrects eq. (12a). However, more important is the consequent correction of the forth term in eq. (9). This term describes heat production. Simple analysis of energy balance shows that the temperature increase in the transitional zone at high  $V$ , when heat losses to surroundings may be neglected, is:

$$\Delta T = T - T_0 = \frac{\sigma(\lambda - 1)}{\rho c} \quad (13)$$

For PET at  $\lambda = 4$   $\Delta T \approx 70^\circ\text{C}$ . The value of  $\Delta T$  is proportional to the product  $(\lambda - 1)\sigma$  and does not depend on  $V$  (at high cross-head speeds). The factor  $(\lambda - 1)$  in eq. (9) is lost. For PET  $\lambda - 1 \approx 3$  and the underestimation of temperature growth by eq. (12b) is 3-fold. For computer calculations Toda multiplied this term by 2.5 to get reasonable temperature in the neck. Fitting parameter of 2.5 corresponds to  $\lambda = 3.5$  that is close to the neck draw ratio of PET. Evidently, for other polymers with different  $\lambda$  eq. (9) is inaccurate. Particularly, for polycarbonate  $\lambda = 1.8$

and eq. (9) at the fitting factor of 2.5 predicts appearance of oscillations while eqs. (8) and (10) predict steady neck propagation in agreement with experimental observations. Thus, there are two inaccuracies in Barenblatt's equations. Toda corrected the first one and the present article corrects the second. It is worth mentioning that eqs. (8) and (10) do not have any fitting parameters.

Self-oscillations appear at high velocities when the draw stress increases with the cross-head speed. This is highly unexpected result. It means that self-oscillations caused by heat instability are essentially different from any other self-oscillations. There are several instability phenomena observed in mechanics, electricity, biology, and chemistry. However, these oscillations may be divided just on few mathematical classes. The heat instability represents the new one and is essentially different from any mechanical instability. Particularly, it contradicts our intuition, and existence of oscillation at high draw velocities is difficult to understand.

Some additional points may be noticed. It is not surprising that testing machine stops recording stress oscillation at high frequencies. However, it happened in the "worst point", at the cross-head speed corresponding to the minimum of the draw stress (Fig. 5). This resulted in erroneous conclusion that the interval of cross-head speeds with oscillatory neck propagation is determined by the criterion of mechanical instability (1).

Inequality (1) does not determine the interval of cross-head speeds where oscillations may appear. It is the necessary condition of oscillatory neck propagation. If it is not fulfilled at least in some interval of cross-head speeds, oscillation in the polymer can not be observed.

In the present work, several essential points were not considered. Particularly, the transition of PET from glassy to rubber-like state and crystallization heat were not taken into account. The transitional zone was assumed very thin. In addition, the reason of appearance of oscillations at high cross-head speeds in PET was not clearly explained. The explanation of oscillations at high cross-head speeds is formally mathematical, and the reason of oscillations remains unclear. The physical nature of the critical length (critical compliance or elastic energy)<sup>17</sup> of sample and relation of the critical length with material properties were not determined. Thus, the theory of oscillatory neck propagation was not developed yet. Despite this, it is clear that the mechanism of self-oscillations is heat instability, and eqs. (8), (10), and (11) may be the foundation of the theory.

In addition, the following point may be mentioned. The heat conductivity of polymers is

~1000-folds lower than that of metals. As a result, the temperature growth in polymers is significant if the neck appears and the testing speed is not very low. For example, an increase of temperature in PET at a cross-head speed of  $V = 10$  mm/min is  $\sim 20^\circ\text{C}$ . This value depends on polymer, but for  $V = 10$  mm/min it is quite typical. Temperature increases both at steady and oscillatory neck propagation. The temperature increase may be neglected only at low cross-head speeds ( $V < 2$  mm/min) when the test time of a sample may exceed an hour.

### CONCLUSIONS

1. The mechanism of self-oscillations is heat instability of neck propagation.
2. Equations describing stress and temperature in a polymer at neck propagation were derived.
3. Neck propagation is oscillatory at high cross-head speeds when the draw stress increases with an increase in cross-head speed.
4. Oscillations in a polymer may be observed if at some cross-head speed Inequality (1) is fulfilled. The interval of oscillations is not described by Inequality (1).
5. Theoretical and experimental values of the critical sample lengths agree.
6. Temperature increase in the neck is proportional to the factor  $(\lambda - 1)$ .

### References

1. Hookway, D. C. *J Text Inst* 1958, 49, 292.
2. Roth, W.; Schroth, R. *Faserforsch Textiltech* 1960, 11, 312.
3. Kechekyan, A. S.; Andrianova, G. P.; Kargin, V. A. *Polym Sci Ser A* 1970, 12, 2424.
4. Roseen, R. *J Mater Sci* 1974, 9, 929.
5. Maher, J. W.; Haward, R. N.; Hay, J. N. *J Polym Sci Polym Phys Ed* 1980, 18, 2169.
6. Toda, A.; Tomita, C.; Hirotsuka, M.; Hibino, Y.; Miyaji, H.; Nonomura, C.; Suzuki, T.; Ishikara, H. *Polymer* 2002, 43, 947.
7. Bazhenov, S. L.; Rodionova, Y. A.; Kechekyan, A. S. *Polym Sci Ser A* 2003, 45, 1099.
8. Pakula, T.; Fischer, E. W. *J Polym Sci Polym Phys Ed* 1981, 19, 1705.
9. Karger-Kocsis, J.; Benevolenski, O. I.; Moskala, E. J. *J Mater Sci* 2001, 36, 3365.
10. Barenblatt, G. I. *Mech Solids* 1970, 5, 110.
11. Bazhenov, S. L.; Kechekyan, A. S. *Polym Sci Ser A* 2001, 43, 63.
12. Bazhenov, S. L.; Kechekyan, A. S. *Polym Sci Ser A* 2002, 44, 629.
13. Toda, A. *Polymer* 1994, 35, 3638.
14. Davidenkov, N. N. *Solid State Phys* 1961, 3, 2458.
15. Godovsky, Y. K. *Thermophysical Properties of Polymers*; Springer: Berlin, 1993.
16. Mikhelson, V. A. *Works, Moscow, Novyi agronom* 1930; Vol. 1, p 319.
17. Boyce, M. C.; Haward, R. N. In *The Physics of Glassy Polymers*; Haward, R. N., Young, R. J., Eds.; Chapman and Hall: London, 1997; p 213.
18. Zeldovich, Y. B.; Barenblatt, G. I.; Librovich, G. I.; Makhviladze, G. M. *Mathematical Theory of Combustion and Explosion*; Nauka: Moscow, 1980.